Chronic RNA G-quadruplex Accumulation in Aging and Alzheimer's Disease

[1]Lena Kallweit, [2]Eric D. Hamlett, [3]Hannah Saternos, [3]Anah Gilmore, *[3]Ann-Charlotte Granholm, *[1]Scott Horowitz

*To whom correspondence should be addressed. These two authors are co-senior authors.

[1]Department of Chemistry & Biochemistry and the Knoebel Institute for Healthy Aging, University of Denver, 2155 E Wesley Ave, Denver, CO 80208, USA.

[2]Department of Pathology and Laboratory Medicine, Medical University of South Carolina, 171 Ashley Avenue, Charleston, SC 29425 USA

[3]Department of Neurosurgery, University of Colorado Anschutz Medical Campus, 12700 East 19th Avenue, P15-5112, Aurora, CO 80045 USA

All figures require color printing.

ABSTRACT

INTRODUCTION: As the world population ages, new molecular targets in aging and Alzheimer's Disease (AD) are needed to combat the expected influx of new AD cases. Until now, the role of RNA structure in aging and neurodegeneration has largely remained unexplored.

METHODS: In this study, we examined human hippocampal *postmortem* tissue for the formation of RNA G-quadruplexes (rG4s) in aging and AD.

RESULTS: We found that rG4 immunostaining strongly increased in the hippocampus with both age and with AD severity. We further found that neurons with accumulation of phospho-tau immunostaining contained rG4s, that rG4 structure can drive tau aggregation, and that rG4 staining density depended on APOE genotype in the human tissue examined.

DISCUSSION: Combined with previous studies showing the dependence of rG4 structure on stress and the extreme power of rG4s at oligomerizing proteins, we propose a model of neurodegeneration in which chronic rG4 formation is linked to proteostasis collapse. These morphological findings suggest that further investigation of RNA structure in neurodegeneration is a critical avenue for future treatments and diagnoses.

1. INTRODUCTION:

As the aged population increases, Alzheimer's Disease (AD) and AD-related dementias (ADRDs) will become one of the world's largest medical and economic crises due to the lack of early diagnostic methods and durable therapies[1, 2]. Age is the highest risk factor for AD, as disease prevalence increases exponentially as a function of age, and close to 40% of older adults over the age of 80 experience AD or ADRDs[3, 4]. The most important genetic risk factor for developing late onset AD (LOAD) is the Apolipoprotein E (APOE) genotype, at least in Caucasians, where carriers of one or two copies of the APOE4 allele have a substantial increase in the risk for developing LOAD when compared to carriers of the APOE2 or 3 alleles[4, 5]. Beyond APOE, recent meta-analyses combining genome-wide association studies (GWAS) have expanded the number of AD-risk loci[6], but most of the disease-associated variants reside in non-protein coding regions of the genome, making it difficult to elucidate how they affect AD susceptibility and pathogenesis.

The exact mechanisms behind these two predominant AD risk factors remains a mystery but both are widely associated with increased abnormal protein aggregation, which is the most abundantly observed pathological hallmark of AD pathogenesis. AD and ADRDs all have an abnormal protein aggregation profile that includes: 1) extracellular amyloid senile plaque deposition occurring at least 5-10 years before mild cognitive impairments (MCI) are observed and, 2) aggregates of phosphorylated Tau (p-Tau) forming intracellular neurofibrillary tangles (NFTs) near MCI onset[7, 8]. Novel biomarker studies have shown that hyperphosphorylated Tau species exist in plasma prior to onset of dementia symptoms, with specific phosphorylation sites seeming to affect the affinity of binding of the Tau protein to microtubules [9]. With advancing age, protein aggregation is accelerated by the accumulation of reactive oxygen species (ROS) as

well as the onset of neuroinflammation in the brain[10-12]. Having APOE4 was shown to significantly increase accumulation of amyloid and NFTs in Caucasians, and also increases inflammation and reactive oxygen species in the human brain[5, 13]. The effects of these AD risk factors have been studied mostly at the protein level in the brain, but not yet at RNA level, where structure and function have a myriad of important roles in numerous biological processes.

RNA higher order structures of particular interest are RNA guanine-rich G-quadruplexes (rG4s)[14]. G-quadruplexes are secondary structures that can fold under physiological conditions by guanine-rich DNA and RNA molecules and occur in the genomes and transcriptomes of many species, including humans[15]. rG4s are four-stranded helices formed by guanine tetrads through Hoogsteen base-pairing, with a monovalent cation channel running down the middle of the tetrads (Fig. 1a)[16]. G4s are potentially involved in the regulation of DNA and RNA processes, such as replication, transcription, translation, RNA localization, and degradation[17-19]. Recently, rG4s were shown to form as a function of stress in eukaryotic cells[20]. Under non-stress conditions, rG4s were largely unfolded, but upon introduction of stress (including ROS stress) the rG4s preferentially folded and remained folded until the cessation of stress[21]. This observation raises the possibility that rG4s could preferentially fold under the increased and chronic stress conditions of aging and AD in the human brain, leading to abnormally high levels of rG4 formation in older adults or in adults with protein misfolding diseases[22]. RNA has been known to be included in AD-related aggregates of both amyloid and NFTs in patients with AD for decades[23], and a recent sequencing study of nucleic acids embedded in AD aggregates showed an enrichment in potential rG4-forming sequences[24].

It has recently been shown that rG4s can greatly enhance protein oligomerization[25, 26]. Moreover, rG4s can bind to and greatly enhance the phase transition of tau[27]. Similarly,

Zwierzchowski-Zarate et al explored the effects of different RNA sequences on tau aggregation in a cellular model[28]. In their study, several sequences caused an increase in tau aggregation, but the highest level of tau aggregation was achieved with a GGGC repeat sequence[28]. However, the structure of the RNAs, including possible rG4 formation, was not explored or speculated upon. We therefore performed CD spectroscopy to determine if the sequence associated with the highest levels of tau fibrillation might be forming rG4 secondary structures. The CD spectra show that this RNA forms parallel rG4 structures *in vitro* (Supplementary Data Fig. 1).

Based on these previous *in vitro* and cellular studies, an increased presence of rG4s in the brain could contribute to AD-associated aggregation. However, the presence of rG4s in the human brain or other human tissues has not been shown previously, nor how it relates to aging or AD pathology. This was the focus of the current study.

2. METHODS:

***Human brain tissue*:** This work was approved by the University of Colorado Institutional Review Board (IRB) and the study was performed in accordance with the ethical standards of the 1964 Declaration of Helsinki and its later amendments. However, the use of *postmortem* brain tissue for research is exempt according to federal IRB regulations and does not require IRB review and approval. All efforts were made to consider diversity, equity and inclusion (DEI) in the selection of brain tissues for this study. The tissues included in this study were obtained from the Medical University of South Carolina (MUSC) brain bank (Dr. Eric Hamlett). *Postmortem* consent was obtained from the next of kin, and the brain was rapidly removed. Fig. 1b shows the demographics for the 21 cases used for this study. The tissue was sliced in 1 cm coronal slices and subjected to free-floating fixation in 4% paraformaldehyde in phosphate buffered saline (PBS) for 72 hours. The fixed tissue was then transferred to a 30% sucrose in phosphate buffer

(PB), followed by transfer to a cryoprotection solution in PBS (30% Glycerol, 30% Ethylene Glycol and 40% PO4 Buffer) and stored in -20^{o} C until dissection. Anatomical blocks from 19 brain regions were dissected from the 1 cm slabs, embedded in paraffin and cut at a thickness of 5µm on a Microm Microtome (Thermo Fisher Scientific Inc., Waltham, MA) and stained for routine neuropathological staging according to the NIA-AA *Revised Criteria for Diagnosis and Staging of Alzheimer's Disease* [29].

Immunofluorescence: Paraffin-embedded sections were deparaffinized in xylene (RPI, CAT#111056) and rehydrated using wash steps at: 100%, 95%, 70%, 50% ethanol followed by distilled water. Heat-induced antigen retrieval was performed using 0.05% citraconic acid at pH 7.2 for 20 minutes in a steamer. Slides were then washed with a saline solution buffered with tris(hydroxymethyl) aminomethane (Tris, TBS) and blocked with 0.25% triton-X and 5% normal serum for 1 hour. After blocking, slides were rinsed again with TBS and incubated with 1X True Black Lipofuscin Autofluorescence Quencher (Biotium CAT#23007) diluted in 70% ethanol. Slides were washed 3 times with TBS then incubated with primary antibodies listed in Supplementary Data Table 1 overnight, followed by Goat anti-mouse AlexaFluor 555 (Thermo Scientific #A32727) or Donkey anti-rabbit Alexafluor 488 (Invitrogen #A-21206) at 1:500 dilution for 1 hour. Slides were then washed 3 times with TBS and cover-slipped using mounting media containing DAPI (Thermo Scientific, CAT#P36931). Staining controls included omission of primary or secondary antibodies (Supplementary Data Fig. 2). In Fig. 3b, we performed sequential double labeling, first with BG4, and then with rRNA antibody at 1:250 (Abcam #ab17119).

In addition, we examined whether Braak stage correlated with aging itself (Supplementary Data Fig. 3). Although not significant at the 0.05 level, there was a weak

correlation between Braak and Age. Braak staging is a paradigm used to describe density and regional spread of neurofibrillary tangles (NFTs) in the Alzheimer brain and includes levels 0-VI [7]. CERAD (Consortium to Establish a Registry for Alzheimer's Disease) is a staging paradigm for Alzheimer's disease that takes into account amyloid plaque formation[30].

Imaging and Statistical methods: Slides were imaged on a confocal microscope at 10X, 20X and 60X magnification at wavelengths 355, 488, and 555. Images used for quantification were taken at constant microscope and intensity settings. All image quantification was performed using Fiji ImageJ. Quantification was performed by a researcher who was blinded to the neuropathological diagnosis of individual cases and with no knowledge of Braak Stage or Age for the case being quantified. Supplemental Table 2 presents side by side comparisons of quantification from 2 researchers who were both blinded to group diagnosis and individual cases. Data used in the paper are highlighted. One data point with too much variation between quantifications was removed to increase rigor. Background was subtracted using a rolling ball radius. Images were then divided into 3 regions of interests (ROI); OML, DG and CA4. (Supplementary Data Fig. 4) Images were submitted to an auto-threshold and particle's analyzed to get a percent area measurement of BG4 staining. These were graphed and linearly fit using Kaleidagraph using Pearson fit. Spearman and Pearson R and p-values are reported for 18 cases for age correlation and 18 cases for Braak correlation. An unpaired T-test with unequal variance was performed for the two groups E2/E3 and E3/E3 vs E3/E4 and E4/E4. When the singular African American case was removed from the APOE quantification, the t-probability remained highly significant at 0.0045 vs 0.002. All quantification was performed on 10X images obtained from an Olympus microscope.

Circular Dichroism: CD spectra were obtained using a Jasco J-1100 circular dichroism at 25°C. Sequence was resuspended in 10mM potassium phosphate pH 7.5 buffer and diluted to 12.5 µM (per strand) RNA. The CD measurement was taken from 300 nm to 210 nm at 1nm intervals using a 50 nm/min scanning speed. The sequence used was 5'-CGGGCGGCGGGGGGGCCCGGGCGGCGGGGGGGCCCGGGCG-3' [28]. Parallel structure was determined using previously described quantification methods for quadruplex topology[31].

3. RESULTS

3.1 Formation of rG4s in aging

To determine if rG4s form in the human brain, we used the well-characterized single-chain BG4 anti- quadruplex antibody (Sigma-Aldrich MABE917, antibody null controls in Supplementary Data Fig. 2) to stain human hippocampal *postmortem* tissue of different ages under conditions that strongly favor cytoplasmic rG4 identification using triton-X fixation in cells [32, 33]. The tissues were obtained in collaboration with the brain bank at the Medical University of South Carolina (MUSC). The study included 21 cases, male and female, of different ages and with or without a clinical or neuropathological diagnosis of AD (see Fig. 1b). All cases had received a neuropathological examination including assessment of Braak and CERAD stages according to the updated NIA criteria except in those cases in which no pathology was noted [7, 34].

First, the rG4 staining profiles were compared between different ages, with an age range of 30-92 years of age (Fig. 1c). We discovered a significant age-related increase in rG4 immunostaining, with the densest staining observed in older individuals (Fig. 1c,d). The largest difference in staining between young and older cases was observed in the outer molecular layer (OML) and in the hilar region, CA4 (see Fig. 1c, legend arrows). The strongest overall staining

for BG4 was found in the dentate gyrus granular cell layer (DG), but with less observable age-related increases. Staining density measurements confirmed these findings and demonstrated a highly significant increase in BG4 staining in the oldest cases studied within the OML (Fig. 1d) and the CA4 regions of cornu ammonis (Supplementary data Fig. 5a), confirming increased intracellular BG4 accumulation as a function of age. Plotting BG4 percent area versus age confirmed the observed findings and showed correlation (Spearman R= 0.49) with high significance (p= 0.038 in the OML region (Fig. 1d). Positive and significant Pearson but not Spearman correlations were observed between age and BG4 area in the CA4 region, Supplementary data Fig. 5a), and non-significant correlations were observed in the dentate granule cell layer. No significant correlation was found with BG4 stain and *postmortem* interval (PMI) (Spearman R = -0.18, p = 0.49 see Supplementary Data Fig. 6). In total, these data show that rG4s increased as a function of age in the human brain. We observed multiple outliers in both older and younger individuals due to Braak stage. For example, an 85-year-old individual with Braak stage 0, or 59-year-old individual with Braak stage 5.5 were outliers as a function of age. This led us to analyze whether rG4 formation increased with Braak stage, a measure of AD severity.

3.2 Formation of rG4*s in AD*

Next, we examined whether the formation of rG4s was associated with AD neuropathology. Braak staging is a neuropathological staging method that takes into account the density of neurofibrillary tangles (NFTs) both within each brain region and also from region to region[30], with higher numerical values representing greater AD severity[7]. Like in the case of aging, increased BG4 staining was readily apparent in AD cases, especially in those cases associated with a higher Braak stage (Fig. 2a). In the OML, plotting BG4 percent area versus

Braak stage demonstrated a strong correlation (Spearman R= 0.72) with highly significantly increased BG4 staining with higher Braak stages (p = 0.00086) (Fig. 2b). Positive significant correlations (R = 0.52, p = 0.028) between Braak stage severity and BG4 staining were also observed within the CA4 region (Supplementary data fig. 4). Interestingly, the OML region is highly involved in AD pathology, and is a hippocampal region where AD pathology is often observed,[35] suggesting that the presence of rG4s in this particular brain region might have significance for amyloid as well as NFT formation during the AD disease process. In addition, a prominent loss of synapses in AD is found in the OML, suggesting a potential close connection with layer 2 of the entorhinal cortex[36].

If rG4 formation is more prevalent in AD than in non-AD cases and directly involved in AD pathology, we would also predict that rG4 formation would be more prevalent in APOE genotypes that are predisposed for higher LOAD risk, i.e. patients with one or two copies of the APOE4 genotype. Indeed, there was a significant (t-probability 0.002) increase in BG4 staining levels in the OML in *postmortem* cases with one or more APOE4 alleles compared to those with only APOE2 or APOE3 alleles (Fig. 2c). This result, although correlative, is consistent with a previous study performed *in vitro* in which the RNA sequences found in aggregates in different APOE genotype cell lines were different[24].

3.3 Patterns of rG4 localization

Images obtained at high magnification using a confocal microscope (Olympus) showed that a large amount of the BG4 immunostaining was localized in the cytoplasm near the nucleus in a punctate pattern, reminiscent of known rG4 formation in vitro and in cell lines in rRNA ribosomal extensions[33]. We therefore also stained with an anti-rRNA antibody to determine whether this was the case in human tissue as well. As expected, the stains overlapped (Fig. 3b,

Fig. S7), showing that at least a large percentage of the observed BG4 signal arose from rG4s and not nuclear DNA G4s. This result also confirms that previously observed rG4 formation in ribosomes[33] also occurs in human brain tissue.

To further explore the formation of rG4s in the human hippocampus, we examined the staining pattern in different cell types based on specific antibody markers. Co-staining with markers for the most common brain cell types, rG4s were clearly abundant in neurons, oligodendrocytes, and astrocytes (Fig. 3c). rG4s exhibited no apparent colocalization with microglia (Fig. 3c). This pattern is especially noticeable in the double labeling with SOX10 (Fig. 3c), which clearly shows the nuclear oligodendrocyte marker SOX10[37] staining in proximity to the cytoplasmic BG4 immunostaining.

We co-stained BG4 with different p-tau epitope antibodies to determine whether pathological aggregation of tau proteins co-occurred with BG4 immunostaining (Fig. 4). Indeed, we found that BG4 immunostaining co-localized with hyper-phosphorylated tau immunostaining in neurons located in the CA1-4 regions of the hippocampus (Fig. 4). We used two different antibodies directed against the serine 396 site (S396) and the threonine 231 (T231) to investigate co-localization with different p-Tau epitopes. Quantifying the percentage of cells co-stained with BG4 and pTau revealed that 85% of the S396 p-tau positive cells also had positive BG4 staining, and 82% of the T231 p-tau positive cells also had positive BG4 staining.

4. DISCUSSION

In this study, we demonstrated that rG4s form preferentially as a function of age and AD pathology in neurons and glial cells the human *postmortem* brain. While the granule cell layer in the dentate gyrus exhibited the most BG4 immunostaining overall, this was not an area most changed with aging and AD, as considerably greater changes were observed in the OML and the

CA4 region of the hippocampus. rG4s were primarily found in the cytoplasm near the nucleus of neurons, astrocytes, and oligodendrocytes and were also found in neurons that contained regions of positive staining against two different epitopes of p-tau. The BG4 staining levels were also impacted by APOE status, with the presence of one or two APOE4 alleles associated with higher BG4 levels in the OML region. The OML is an interesting region of the hippocampus from the pathology standpoint, since this is the region of the hippocampus exhibiting the most prominent synaptic loss early in the disease process[36, 38]. We have recently demonstrated a significant loss of presynaptic components of the OML in AD[38], strengthening the findings observed herein and suggesting a particular vulnerability of this region of the hippocampus to AD progressive pathology.

Combining these observations with those previously made on the reliance of rG4 structure on cellular stress and the roles of rG4s in protein oligomerization and tau aggregation *in vitro*, we can propose a model of how rG4s form and could perpetuate the effects of AD (Fig. 4c). As ROS and other protein stresses accumulate with age and according to APOE genotype, rG4s form. Although rG4s can rescue protein folding and could release proteins when unfolded at stress cessation[39], under persistent stress proteins RNA would not be released from the G-quadruplexes, leading to increased protein oligomerization and aggregation[26]. This function has previously been suggested for RNA in biomolecular condensates more generally[40]. The acceleration of protein oligomerization and aggregation by the rG4s could then contribute to a vicious cycle of increased aggregation, leading to synaptic loss as described recently for the OML[38]. Recent in vitro work confirms an interaction between rG4 formation and p-Tau aggregation specifically[41]. In vitro experiments focused on the specific mechanisms for the rG4 influence on Tau phosphorylation and/or aggregation will be an important future focus following

these preliminary observations to more clearly delineate roles of rG4s in neurodegeneration. Of note, the previous studies showing that the fixation conditions used here strongly favor rG4 identification instead of DNA G4 identification were performed in cells, and so it is possible that in tissue some DNA staining could also occur, however this is not suggested by the co-stain with rRNA (Fig. 3b).

Of note, the accumulation or rG4s in neurodegeneration could have roles in addition to those of protein aggregation. RNA transport dysregulation has also been a common factor identified in neurodegeneration[42], and it could be possible that the rG4 build-up observed here could be in part a product of this process or could lead to it. It has also been proposed that the RNA transport dysregulation and protein aggregation processes could be linked [43]. This remains an area of needed future investigation.

This work raises the possibility of using rG4s as potential drug targets in AD, or given the high correlation with AD severity, as early AD biomarkers. Future work can focus on ameliorating AD symptoms through rG4 binding molecules or detecting brain-derived rG4s as disease biomarkers for diagnosis. Many different rG4-binding molecules have already been created and shown to bind in human cells[44], and provide a set of promising lead compounds for potential AD treatment.

Although here we have examined only AD, there are many other aging-related diseases featuring protein aggregation, including Parkinson's Disease, ALS, Fragile X syndrome, and Huntington's Disease [45]. Notably, all of these diseases now have significant evidence showing rG4s as interactors with the aggregating proteins [46-58], and in the case of Fragile X, a recent study demonstrated that rG4s could contribute to its aggregation and neurotoxicity[59]. In addition, a recent manuscript by Raguseo et al., showed an increased prevalence of G4-structures in

C9orf72 mutant human motor neurons in ALS/FTD when compared to healthy motor neurons, and direct involvement of the rG4 complex in the aggregation process[60] . These recent findings illustrate the need to explore rG4 complexes and their role in neurodegeneration further. The results here combined with these previous studies suggest that the formation of rG4s could be a common mechanism of neurodegeneration.

References

1. Collaborators GBDN. Global, regional, and national burden of neurological disorders, 1990-2016: a systematic analysis for the Global Burden of Disease Study 2016. Lancet Neurol. 2019;18(5):459-80. Epub 20190314. doi: 10.1016/S1474-4422(18)30499-X. PubMed PMID: 30879893; PMCID: PMC6459001.
2. Breijyeh Z, Karaman R. Comprehensive Review on Alzheimer's Disease: Causes and Treatment. Molecules. 2020;25(24). Epub 20201208. doi: 10.3390/molecules25245789. PubMed PMID: 33302541; PMCID: PMC7764106.
3. R AA. Risk factors for Alzheimer's disease. Folia Neuropathol. 2019;57(2):87-105. doi: 10.5114/fn.2019.85929. PubMed PMID: 31556570.
4. Hersi M, Irvine B, Gupta P, Gomes J, Birkett N, Krewski D. Risk factors associated with the onset and progression of Alzheimer's disease: A systematic review of the evidence. Neurotoxicology. 2017;61:143-87. Epub 20170329. doi: 10.1016/j.neuro.2017.03.006. PubMed PMID: 28363508.
5. Bejanin A, Iulita MF, Vilaplana E, Carmona-Iragui M, Benejam B, Videla L, Barroeta I, Fernandez S, Altuna M, Pegueroles J, Montal V, Valldeneu S, Gimenez S, Gonzalez-Ortiz S, Munoz L, Padilla C, Aranha MR, Estelles T, Illan-Gala I, Belbin O, Camacho V, Wilson LR, Annus T, Osorio RS, Videla S, Lehmann S, Holland AJ, Zetterberg H, Blennow K, Alcolea D, Clarimon J, Zaman SH, Blesa R, Lleo A, Fortea J. Association of Apolipoprotein E varepsilon4 Allele With Clinical and Multimodal Biomarker Changes of Alzheimer Disease in Adults With Down Syndrome. JAMA Neurol. 2021;78(8):937-47. doi: 10.1001/jamaneurol.2021.1893. PubMed PMID: 34228042; PMCID: PMC8261691.
6. Novikova G, Andrews SJ, Renton AE, Marcora E. Beyond association: successes and challenges in linking non-coding genetic variation to functional consequences that modulate Alzheimer's disease risk. Mol Neurodegener. 2021;16(1):27. Epub 20210421. doi: 10.1186/s13024-021-00449-0. PubMed PMID: 33882988; PMCID: PMC8061035.
7. Braak H, Braak E. Staging of Alzheimer's disease-related neurofibrillary changes. Neurobiol Aging. 1995;16(3):271-8; discussion 8-84. Epub 1995/05/01. doi: 10.1016/0197-4580(95)00021-6. PubMed PMID: 7566337.
8. Furman JL, Vaquer-Alicea J, White CL, 3rd, Cairns NJ, Nelson PT, Diamond MI. Widespread tau seeding activity at early Braak stages. Acta Neuropathol. 2017;133(1):91-100. doi: 10.1007/s00401-016-1644-z. PubMed PMID: 27878366.

9. Gonzalez-Ortiz F, Kac PR, Brum WS, Zetterberg H, Blennow K, Karikari TK. Plasma phospho-tau in Alzheimer's disease: towards diagnostic and therapeutic trial applications. Mol Neurodegener. 2023;18(1):18. Epub 20230316. doi: 10.1186/s13024-023-00605-8. PubMed PMID: 36927491; PMCID: PMC10022272.

10. Bennett RE, DeVos SL, Dujardin S, Corjuc B, Gor R, Gonzalez J, Roe AD, Frosch MP, Pitstick R, Carlson GA, Hyman BT. Enhanced Tau Aggregation in the Presence of Amyloid beta. Am J Pathol. 2017;187(7):1601-12. Epub 2017/05/14. doi: 10.1016/j.ajpath.2017.03.011. PubMed PMID: 28500862; PMCID: PMC5500829.

11. Ibanez-Salazar A, Banuelos-Hernandez B, Rodriguez-Leyva I, Chi-Ahumada E, Monreal-Escalante E, Jimenez-Capdeville ME, Rosales-Mendoza S. Oxidative Stress Modifies the Levels and Phosphorylation State of Tau Protein in Human Fibroblasts. Front Neurosci. 2017;11:495. Epub 20170907. doi: 10.3389/fnins.2017.00495. PubMed PMID: 28936161; PMCID: PMC5594088.

12. Leng F, Edison P. Neuroinflammation and microglial activation in Alzheimer disease: where do we go from here? Nat Rev Neurol. 2021;17(3):157-72. Epub 20201214. doi: 10.1038/s41582-020-00435-y. PubMed PMID: 33318676.

13. Raber J, Huang Y, Ashford JW. ApoE genotype accounts for the vast majority of AD risk and AD pathology. Neurobiol Aging. 2004;25(5):641-50. doi: 10.1016/j.neurobiolaging.2003.12.023. PubMed PMID: 15172743.

14. Dumas L, Herviou P, Dassi E, Cammas A, Millevoi S. G-Quadruplexes in RNA Biology: Recent Advances and Future Directions. Trends Biochem Sci. 2021;46(4):270-83. Epub 20201207. doi: 10.1016/j.tibs.2020.11.001. PubMed PMID: 33303320.

15. Rouleau S, Jodoin R, Garant JM, Perreault JP. RNA G-Quadruplexes as Key Motifs of the Transcriptome. Adv Biochem Eng Biotechnol. 2020;170:1-20. doi: 10.1007/10_2017_8. PubMed PMID: 28382477.

16. Lyu K, Chow EY, Mou X, Chan TF, Kwok CK. RNA G-quadruplexes (rG4s): genomics and biological functions. Nucleic Acids Res. 2021;49(10):5426-50. doi: 10.1093/nar/gkab187. PubMed PMID: 33772593; PMCID: PMC8191793.

17. Bryan TM. Mechanisms of DNA Replication and Repair: Insights from the Study of G-Quadruplexes. Molecules. 2019;24(19). Epub 20190922. doi: 10.3390/molecules24193439. PubMed PMID: 31546714; PMCID: PMC6804030.

18. Kejnovsky E, Tokan V, Lexa M. Transposable elements and G-quadruplexes. Chromosome Res. 2015;23(3):615-23. doi: 10.1007/s10577-015-9491-7. PubMed PMID: 26403244.

19. Yuan WF, Wan LY, Peng H, Zhong YM, Cai WL, Zhang YQ, Ai WB, Wu JF. The influencing factors and functions of DNA G-quadruplexes. Cell Biochem Funct. 2020;38(5):524-32. Epub 20200213. doi: 10.1002/cbf.3505. PubMed PMID: 32056246; PMCID: PMC7383576.

20. Nakanishi C, Seimiya H. G-quadruplex in cancer biology and drug discovery. Biochem Biophys Res Commun. 2020;531(1):45-50. Epub 20200417. doi: 10.1016/j.bbrc.2020.03.178. PubMed PMID: 32312519.

21. Kharel P, Fay M, Manasova EV, Anderson PJ, Kurkin AV, Guo JU, Ivanov P. Stress promotes RNA G-quadruplex folding in human cells. Nat Commun. 2023;14(1):205. Epub 20230113. doi: 10.1038/s41467-023-35811-x. PubMed PMID: 36639366; PMCID: PMC9839774.

22. Vijay Kumar MJ, Morales R, Tsvetkov AS. G-quadruplexes and associated proteins in aging and Alzheimer's disease. Front Aging. 2023;4:1164057. Epub 20230601. doi: 10.3389/fragi.2023.1164057. PubMed PMID: 37323535; PMCID: PMC10267416.
23. Wolozin B, Apicco D. RNA binding proteins and the genesis of neurodegenerative diseases. Adv Exp Med Biol. 2015;822:11-5. doi: 10.1007/978-3-319-08927-0_3. PubMed PMID: 25416971; PMCID: PMC4694570.
24. Shmookler Reis RJ, Atluri R, Balasubramaniam M, Johnson J, Ganne A, Ayyadevara S. "Protein aggregates" contain RNA and DNA, entrapped by misfolded proteins but largely rescued by slowing translational elongation. Aging Cell. 2021:e13326. Epub 2021/04/01. doi: 10.1111/acel.13326. PubMed PMID: 33788386.
25. Masai H, Fukatsu R, Kakusho N, Kanoh Y, Moriyama K, Ma Y, Iida K, Nagasawa K. Rif1 promotes association of G-quadruplex (G4) by its specific G4 binding and oligomerization activities. Sci Rep. 2019;9(1):8618. Epub 20190613. doi: 10.1038/s41598-019-44736-9. PubMed PMID: 31197198; PMCID: PMC6565636.
26. Begeman A, Son A, Litberg TJ, Wroblewski TH, Gehring T, Huizar Cabral V, Bourne J, Xuan Z, Horowitz S. G-Quadruplexes act as sequence-dependent protein chaperones. EMBO Rep. 2020:e49735. Epub 2020/09/19. doi: 10.15252/embr.201949735. PubMed PMID: 32945124.
27. Yasushi Y, Kazuya M, Ginji K, Kenta K, Karin H, Susumu I, Yasushi K, Tomohiro M, Norifumi S. RNA G-quadruplexes and calcium ions synergistically induce Tau phase transition <em>in vitro</em&gt. bioRxiv. 2024:2024.03.01.582861. doi: 10.1101/2024.03.01.582861.
28. Zwierzchowski-Zarate AN, Mendoza-Oliva A, Kashmer OM, Collazo-Lopez JE, White CL, 3rd, Diamond MI. RNA induces unique tau strains and stabilizes Alzheimer's disease seeds. J Biol Chem. 2022;298(8):102132. Epub 20220611. doi: 10.1016/j.jbc.2022.102132. PubMed PMID: 35700826; PMCID: PMC9364032.
29. Hyman BT, Phelps CH, Beach TG, Bigio EH, Cairns NJ, Carrillo MC, Dickson DW, Duyckaerts C, Frosch MP, Masliah E, Mirra SS, Nelson PT, Schneider JA, Thal DR, Thies B, Trojanowski JQ, Vinters HV, Montine TJ. National Institute on Aging-Alzheimer's Association guidelines for the neuropathologic assessment of Alzheimer's disease. Alzheimers Dement. 2012;8(1):1-13. doi: 10.1016/j.jalz.2011.10.007. PubMed PMID: 22265587; PMCID: PMC3266529.
30. Trejo-Lopez JA, Yachnis AT, Prokop S. Neuropathology of Alzheimer's Disease. Neurotherapeutics. 2022;19(1):173-85. Epub 20211102. doi: 10.1007/s13311-021-01146-y. PubMed PMID: 34729690; PMCID: PMC9130398.
31. Cheng M, Cheng Y, Hao J, Jia G, Zhou J, Mergny JL, Li C. Loop permutation affects the topology and stability of G-quadruplexes. Nucleic Acids Res. 2018;46(18):9264-75. doi: 10.1093/nar/gky757. PubMed PMID: 30184167; PMCID: PMC6182180.
32. Laguerre A, Wong JM, Monchaud D. Direct visualization of both DNA and RNA quadruplexes in human cells via an uncommon spectroscopic method. Sci Rep. 2016;6:32141. Epub 20160818. doi: 10.1038/srep32141. PubMed PMID: 27535322; PMCID: PMC4989495.
33. Mestre-Fos S, Ito C, Moore CM, Reddi AR, Williams LD. Human ribosomal G-quadruplexes regulate heme bioavailability. J Biol Chem. 2020;295(44):14855-65. Epub 20200813. doi: 10.1074/jbc.RA120.014332. PubMed PMID: 32817343; PMCID: PMC7606673.

34. Jack CR, Jr., Knopman DS, Weigand SD, Wiste HJ, Vemuri P, Lowe V, Kantarci K, Gunter JL, Senjem ML, Ivnik RJ, Roberts RO, Rocca WA, Boeve BF, Petersen RC. An operational approach to National Institute on Aging-Alzheimer's Association criteria for preclinical Alzheimer disease. Ann Neurol. 2012;71(6):765-75. doi: 10.1002/ana.22628. PubMed PMID: 22488240; PMCID: PMC3586223.

35. Dong H, Martin MV, Chambers S, Csernansky JG. Spatial relationship between synapse loss and beta-amyloid deposition in Tg2576 mice. J Comp Neurol. 2007;500(2):311-21. doi: 10.1002/cne.21176. PubMed PMID: 17111375; PMCID: PMC1661843.

36. Lassmann H, Fischer P, Jellinger K. Synaptic pathology of Alzheimer's disease. Ann N Y Acad Sci. 1993;695:59-64. doi: 10.1111/j.1749-6632.1993.tb23028.x. PubMed PMID: 8239314.

37. Turnescu T, Arter J, Reiprich S, Tamm ER, Waisman A, Wegner M. Sox8 and Sox10 jointly maintain myelin gene expression in oligodendrocytes. Glia. 2018;66(2):279-94. Epub 20171011. doi: 10.1002/glia.23242. PubMed PMID: 29023979.

38. Haytural H, Jorda-Siquier T, Winblad B, Mulle C, Tjernberg LO, Granholm AC, Frykman S, Barthet G. Distinctive alteration of presynaptic proteins in the outer molecular layer of the dentate gyrus in Alzheimer's disease. Brain Commun. 2021;3(2):fcab079. Epub 20210513. doi: 10.1093/braincomms/fcab079. PubMed PMID: 34013204; PMCID: PMC8117432.

39. Son A, Huizar Cabral V, Huang Z, Litberg TJ, Horowitz S. G-quadruplexes rescuing protein folding. Proc Natl Acad Sci U S A. 2023;120(20):e2216308120. Epub 20230508. doi: 10.1073/pnas.2216308120. PubMed PMID: 37155907; PMCID: PMC10194009.

40. Mateju D, Franzmann TM, Patel A, Kopach A, Boczek EE, Maharana S, Lee HO, Carra S, Hyman AA, Alberti S. An aberrant phase transition of stress granules triggered by misfolded protein and prevented by chaperone function. Embo J. 2017;36(12):1669-87. doi: 10.15252/embj.201695957. PubMed PMID: WOS:000403276700005.

41. Yabuki Y, Matsuo K, Komiya G, Kudo K, Hori K, Ikenoshita S, Kawata Y, Mizobata T, Shioda N. RNA G-quadruplexes and calcium ions synergistically induce Tau phase transition in vitro. bioRxiv. 2024:2024.03.01.582861. doi: 10.1101/2024.03.01.582861.

42. Fernandopulle MS, Lippincott-Schwartz J, Ward ME. RNA transport and local translation in neurodevelopmental and neurodegenerative disease. Nat Neurosci. 2021;24(5):622-32. Epub 20210128. doi: 10.1038/s41593-020-00785-2. PubMed PMID: 33510479; PMCID: PMC8860725.

43. Bitetto G, Di Fonzo A. Nucleo-cytoplasmic transport defects and protein aggregates in neurodegeneration. Transl Neurodegener. 2020;9(1):25. Epub 20200703. doi: 10.1186/s40035-020-00205-2. PubMed PMID: 32616075; PMCID: PMC7333321.

44. Zheng BX, Yu J, Long W, Chan KH, Leung ASL, Wong WL. Structurally diverse G-quadruplexes as the noncanonical nucleic acid drug target for live cell imaging and antibacterial study. Chem Commun. 2023;59(11):1415-33. doi: 10.1039/d2cc05945b. PubMed PMID: WOS:000912801300001.

45. Ross CA, Poirier MA. Protein aggregation and neurodegenerative disease. Nat Med. 2004;10 Suppl:S10-7. doi: 10.1038/nm1066. PubMed PMID: 15272267.

46. Imperatore JA, McAninch DS, Valdez-Sinon AN, Bassell GJ, Mihailescu MR. FUS Recognizes G Quadruplex Structures Within Neuronal mRNAs. Front Mol Biosci. 2020;7:6. Epub 2020/03/03. doi: 10.3389/fmolb.2020.00006. PubMed PMID: 32118033; PMCID: PMC7018707.

47. Ishiguro A, Kimura N, Noma T, Shimo-Kon R, Ishihama A, Kon T. Molecular dissection of ALS-linked TDP-43 - involvement of the Gly-rich domain in interaction with G-quadruplex mRNA.

FEBS Lett. 2020;594(14):2254-65. Epub 2020/04/28. doi: 10.1002/1873-3468.13800. PubMed PMID: 32337711.

48. Liu X, Xu Y. HnRNPA1 Specifically Recognizes the Base of Nucleotide at the Loop of RNA G-Quadruplex. Molecules. 2018;23(1). Epub 2018/01/25. doi: 10.3390/molecules23010237. PubMed PMID: 29361764; PMCID: PMC6017123.

49. Mori K, Lammich S, Mackenzie IR, Forne I, Zilow S, Kretzschmar H, Edbauer D, Janssens J, Kleinberger G, Cruts M, Herms J, Neumann M, Van Broeckhoven C, Arzberger T, Haass C. hnRNP A3 binds to GGGGCC repeats and is a constituent of p62-positive/TDP43-negative inclusions in the hippocampus of patients with C9orf72 mutations. Acta Neuropathol. 2013;125(3):413-23. Epub 2013/02/06. doi: 10.1007/s00401-013-1088-7. PubMed PMID: 23381195.

50. Oyoshi T, Kurokawa R. Structure of noncoding RNA is a determinant of function of RNA binding proteins in transcriptional regulation. Cell Biosci. 2012;2(1):1. Epub 2012/01/05. doi: 10.1186/2045-3701-2-1. PubMed PMID: 22214309; PMCID: PMC3274451.

51. Scalabrin M, Frasson I, Ruggiero E, Perrone R, Tosoni E, Lago S, Tassinari M, Palu G, Richter SN. The cellular protein hnRNP A2/B1 enhances HIV-1 transcription by unfolding LTR promoter G-quadruplexes. Sci Rep. 2017;7:45244. Epub 2017/03/25. doi: 10.1038/srep45244. PubMed PMID: 28338097; PMCID: PMC5364415.

52. Takahama K, Kino K, Arai S, Kurokawa R, Oyoshi T. Identification of Ewing's sarcoma protein as a G-quadruplex DNA- and RNA-binding protein. FEBS J. 2011;278(6):988-98. Epub 2011/01/20. doi: 10.1111/j.1742-4658.2011.08020.x. PubMed PMID: 21244633.

53. Liu W, Xu Y, Li X, Meng Y, Wang H, Liu C, Liu C, Wang L. A DNA G-quadruplex converts SOD1 into fibrillar aggregates. Chinese Chemical Letters. 2021. doi: https://doi.org/10.1016/j.cclet.2021.01.045.

54. Mejzini R, Flynn LL, Pitout IL, Fletcher S, Wilton SD, Akkari PA. ALS Genetics, Mechanisms, and Therapeutics: Where Are We Now? Front Neurosci. 2019;13:1310. Epub 20191206. doi: 10.3389/fnins.2019.01310. PubMed PMID: 31866818; PMCID: PMC6909825.

55. Guerrero EN, Wang H, Mitra J, Hegde PM, Stowell SE, Liachko NF, Kraemer BC, Garruto RM, Rao KS, Hegde ML. TDP-43/FUS in motor neuron disease: Complexity and challenges. Prog Neurobiol. 2016;145-146:78-97. Epub 2016/10/04. doi: 10.1016/j.pneurobio.2016.09.004. PubMed PMID: 27693252; PMCID: PMC5101148.

56. Riccardi C, D'Aria F, Digilio FA, Carillo MR, Amato J, Fasano D, De Rosa L, Paladino S, Melone MAB, Montesarchio D, Giancola C. Fighting the Huntington's Disease with a G-Quadruplex-Forming Aptamer Specifically Binding to Mutant Huntingtin Protein: Biophysical Characterization, In Vitro and In Vivo Studies. Int J Mol Sci. 2022;23(9). Epub 20220427. doi: 10.3390/ijms23094804. PubMed PMID: 35563194; PMCID: PMC9101412.

57. Goering R, Hudish LI, Guzman BB, Raj N, Bassell GJ, Russ HA, Dominguez D, Taliaferro JM. FMRP promotes RNA localization to neuronal projections through interactions between its RGG domain and G-quadruplex RNA sequences. Elife. 2020;9. doi: ARTN e52621 10.7554/eLife.52621. PubMed PMID: WOS:000541416100001.

58. Matsuo K, Asamitsu S, Maeda K, Kawakubo K, Komiya G, Kudo K, Sakai Y, Hori K, Ikenoshita S, Usuki S, Funahashi S, Kawata Y, Mizobata T, Shioda N, Yabuki Y. RNA G-quadruplexes forming scaffolds for α-synuclein aggregation lead to progressive neurodegeneration. bioRxiv. 2023:2023.07.10.548322. doi: 10.1101/2023.07.10.548322.

59. Asamitsu S, Yabuki Y, Ikenoshita S, Kawakubo K, Kawasaki M, Usuki S, Nakayama Y, Adachi K, Kugoh H, Ishii K, Matsuura T, Nanba E, Sugiyama H, Fukunaga K, Shioda N. CGG repeat RNA G-quadruplexes interact with FMRpolyG to cause neuronal dysfunction in fragile X-related tremor/ataxia syndrome. Sci Adv. 2021;7(3). Epub 20210113. doi: 10.1126/sciadv.abd9440. PubMed PMID: 33523882; PMCID: PMC7806243.

60. Raguseo F, Wang Y, Li J, Petric Howe M, Balendra R, Huyghebaert A, Vadukul DM, Tanase DA, Maher TE, Malouf L, Rubio-Sanchez R, Aprile FA, Elani Y, Patani R, Di Michele L, Di Antonio M. The ALS/FTD-related C9orf72 hexanucleotide repeat expansion forms RNA condensates through multimolecular G-quadruplexes. Nat Commun. 2023;14(1):8272. Epub 20231213. doi: 10.1038/s41467-023-43872-1. PubMed PMID: 38092738; PMCID: PMC10719400.

Acknowledgements: Funding for this project was provided by NIH R35GM142442 to S.H., and NIH 5R01AG071228-02, R01AG070153, and R01AG061566 as well as a grant from the BrightFocus Foundation (CA2018010) to A.C.G.

Author Contributions: Idea generated by S.H., work conceptualized by S.H. and A.C.G. Experiments designed by S.H. and A.C.G, with assistance from all authors. Tissues collected and catalogued by E.D.H. Experiments performed by L.K., with assistance from H.S. and A.G. Primary writing performed by S.H., A.G.G., and L.K., with editing provided by all authors.

Authors declare no competing interests.

Keywords: quadruplex, RNA, Alzheimer’s, aggregation, tau, ApoE

Figures:

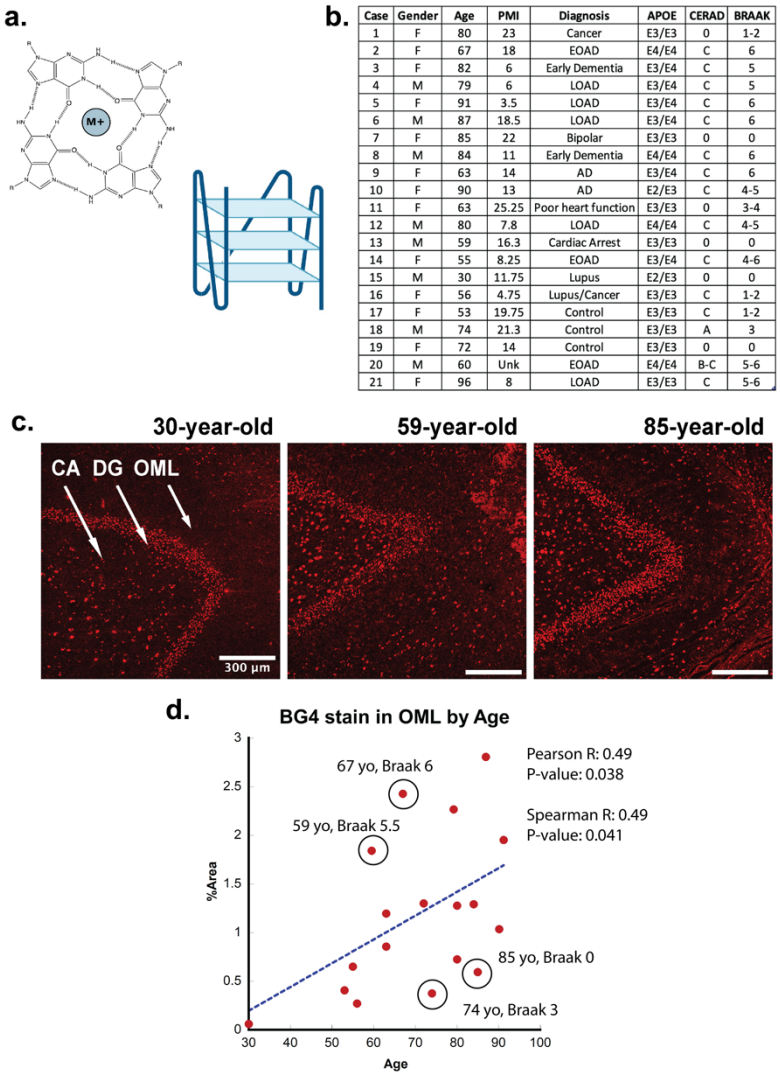

Case	Gender	Age	PMI	Diagnosis	APOE	CERAD	BRAAK
1	F	80	23	Cancer	E3/E3	0	1-2
2	F	67	18	EOAD	E4/E4	C	6
3	F	82	6	Early Dementia	E3/E4	C	5
4	M	79	6	LOAD	E3/E4	C	5
5	F	91	3.5	LOAD	E3/E4	C	6
6	M	87	18.5	LOAD	E3/E4	C	6
7	F	85	22	Bipolar	E3/E3	0	0
8	M	84	11	Early Dementia	E4/E4	C	6
9	F	63	14	AD	E3/E4	C	6
10	F	90	13	AD	E2/E3	C	4-5
11	F	63	25.25	Poor heart function	E3/E3	0	3-4
12	M	80	7.8	LOAD	E4/E4	C	4-5
13	M	59	16.3	Cardiac Arrest	E3/E3	0	0
14	F	55	8.25	EOAD	E3/E4	C	4-6
15	M	30	11.75	Lupus	E2/E3	0	0
16	F	56	4.75	Lupus/Cancer	E3/E3	C	1-2
17	F	53	19.75	Control	E3/E3	C	1-2
18	M	74	21.3	Control	E3/E3	A	3
19	F	72	14	Control	E3/E3	0	0
20	M	60	Unk	EOAD	E4/E4	B-C	5-6
21	F	96	8	LOAD	E3/E3	C	5-6

Fig 1. a, (left) Representative G-quadruplex tetrad structure with Hoogsteen base pairing stabilized by a cation at the center. (right) G-quadruplex structure with stacked tetrads. **b**, Demographics table for individuals included in this study. **c**, Immunofluorescence showing BG4 staining (red) in brain sections of human hippocampus from four control individuals of increasing age ranging 30-91 years old (Case 15, 13, and 8, respectively) all with Braak stage 0. **d**, Correlation of percent area covered by BG4 fluorescence in the outer-molecular layer versus age of individual.

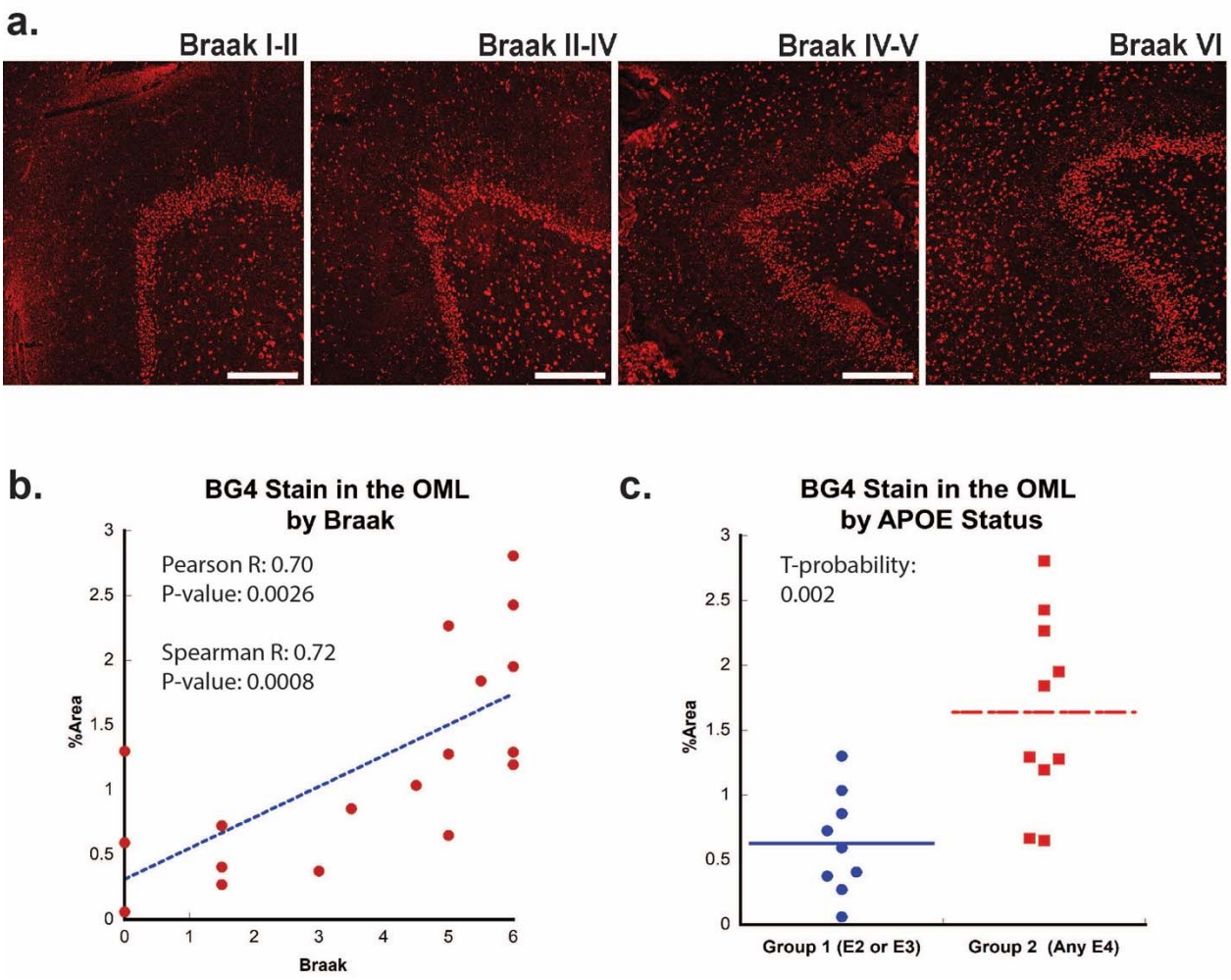

Fig 2. a, Immunofluorescence showing BG4 staining (red) in brain sections of human hippocampus with increasing Braak stage (1-6) associated with AD severity (Case 16, 11, 10, and 8, respectively). All scale bars are 300 µm. b, Correlation of percent area BG4 coverage in the outer molecular layer versus severity of Braak stage. **c**, Quantification of percent area BG4 coverage by population with E2/E3 and E3/E3 versus E3/E4 and E4/E4 APOE alleles.

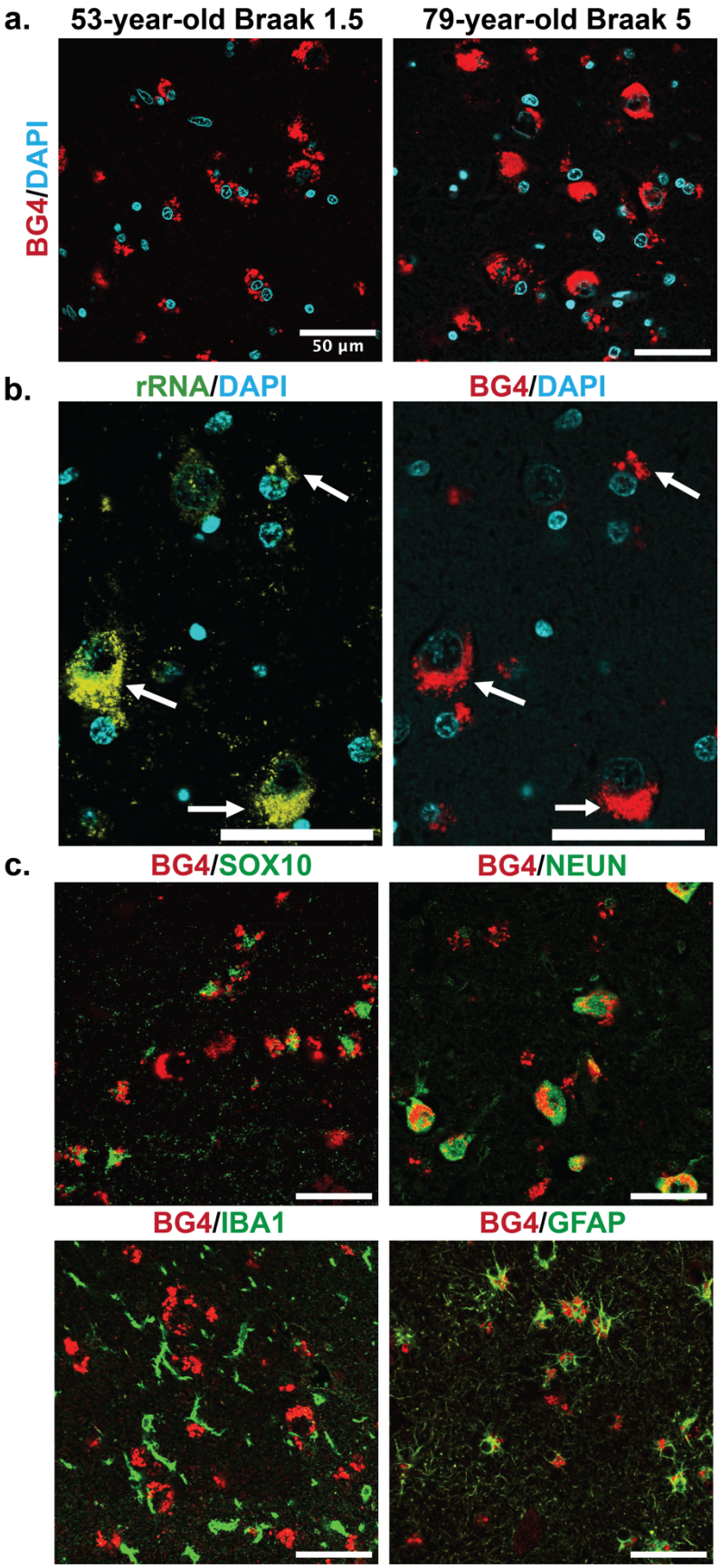

Fig 3. Cellular types and localization of rG4s, all scale bars are 50 µm. **a**, Immunofluorescence showing BG4 staining patterns (red) in human hippocampal tissue of case 17, a 53-year-old individual with Braak stage 1.5, and case 4, a 79-year-old individual with Braak stage 5 AD pathology (right). Cell nuclei stained with DAPI (blue). **b**, Co-stain of rRNA (left, yellow green) and BG4 (right, red), in the hippocampal CA4 region, an 80-year old individual with early stage tauopathy, demonstrating significant but not complete overlap between BG4 and rRNA. **c**, BG4 staining (red) with cell type markers (green) of oligodendrocytes (SOX10, case 8), neurons (NEUN, case 4), microglia (IBA1, case 18) and astrocytes (GFAP, case 18). BG4 is most prevalent in oligodendrocytes, neurons, and astrocytes. BG4 does not strongly colocalize with microglia (IBA1).

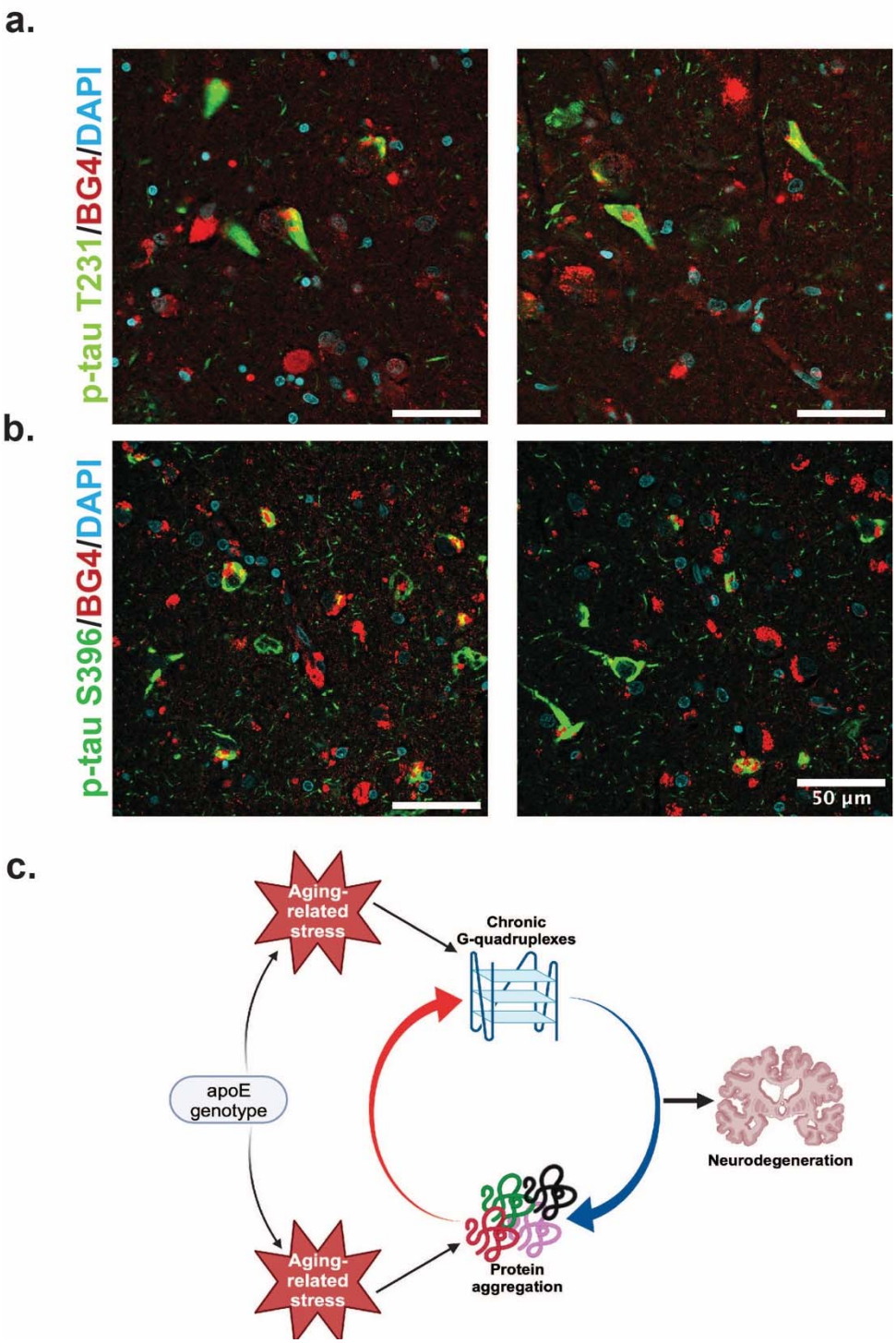

Fig 4. Colocalization of rG4s with p-tau and neurodegeneration model. a, Immunofluorescence of human hippocampus from 2 older AD individuals (case 8 and case 21)showing BG4 (red), DAPI (blue), and p-tau (green). **b**, Proposed model relating chronic rG4 formation and protein aggregation in aging and neurodegeneration.